

Recovery in deformed copper and nickel single crystals

R. E. COOK, G. GOTTSTEIN*, U. F. KOCKS[‡]

Materials Science Division, Argonne National Laboratory, Argonne, IL 60439, USA

The static recovery behaviour of copper and nickel single crystals deformed in multiple slip was investigated in mechanical tests and in HVEM *in situ* annealing experiments. Recovery of Type I, as previously identified in aluminium was observed in both its microscopic and macroscopic features: a sharpening of the cell-wall structure without a change in substructure scale, correlated with a short transient in the strain-hardening behaviour during retesting. The substructure development with increasing recovery time and temperature is similar to that during dynamic recovery, i.e. with increasing strain in a continuous test. After longer recovery times or at higher annealing temperatures, the specimens recrystallize; after larger strains, they recrystallize dynamically. An intermediate stage akin to the Type II recovery found in aluminium was never observed, either in its macroscopic manifestation of a long reloading transient, or as a general coarsening of the subgrain structure. Examples of local sub-boundary mobility and dissolution were, however, seen in situations close to static or dynamic recrystallization. It is concluded that the fluctuations occurring during subgrain coarsening are stable in aluminium, leading to Type II recovery and extended steady-state deformation, but unstable in copper and nickel, leading to static or dynamic recrystallization.

1. Introduction

Recovery from the deformed state is an especially important phenomenon when it occurs simultaneously with deformation: dynamic recovery controls steady-state creep and the large-strain forming resistance [1], and is, under some circumstances, a necessary precursor to recrystallization [2]. The mechanism of dynamic recovery appears to be related to that of static recovery (the classical effect of high-temperature annealing on low-temperature stress/strain behaviour), even though static recovery at the deformation temperature proceeds much more slowly than dynamic recovery [3, 4].

To isolate recovery from deformation mechanisms, it is particularly opportune to study static recovery. Such static recovery has been widely

investigated [5-9] and reviewed [10, 11]. The general result is that metals with high stacking fault energy (SFE) show strong recovery and a well developed polygonized microstructure, while recovery is sometimes difficult to observe in metals with low SFE. One reason for this difference could be that dynamic recrystallization (DRX) tends to intervene in low-SFE metals and limit the range of strains for homogeneous deformation [12, 13].

A more detailed investigation of recovery mechanisms, with respect to both microstructural changes and macroscopic mechanical behaviour, has recently been undertaken in aluminium single crystals of a $\langle 111 \rangle$ orientation[†], which were compressed at room temperature ($T_m/3$) and annealed at $T_m/2$ [3, 16]. As a result, Hasegawa

*Present address: Institut für Allg. Metallkunde und Metallphysik, RWTH Aachen, W. Germany.

[‡]Present address: The Center for Materials Science, Los Alamos National Laboratory, Los Alamos, New Mexico 87545, USA.

[†]Physical mechanisms are often better investigated in single crystals; however, it is essential that the deformation be in multiple slip, if the observed behaviour is to have any relevance to that of grains in polycrystals [14, 15].

and Kocks [3] identified two types of recovery: a "Type I", which corresponds to a tightening of the deformation-generated cell walls into sub-boundaries and leads to but small transients in subsequent strain-hardening behaviour; and a "Type II", which corresponds to a coarsening of the subgrain structure and alters the subsequent stress/strain behaviour significantly, for relatively large strains. It was shown that this classification was more appropriate than the classical one into "ortho-" and "meta-"recovery [17, 18], which are both of Type I; and it was speculated that there might be a connection between Type II recovery and the "in situ recrystallization" observed in copper [19], silver [20] and nickel [21] at high temperatures.

The intent of the present investigation was to ascertain whether the recovery behaviour of copper and nickel single crystals, after deformation in multiple slip, could also be classified into Type I and Type II, by its macroscopic and/or microscopic characteristics. Since both copper and nickel exhibit dynamic recrystallization (DRX) [21], it is especially important to study single crystals: the absence of grain boundaries delays DRX [22, 23]. On the other hand, the possibility of studying any interaction or competition between recovery (especially of Type II) and DRX offers an additional incentive. In a preceding paper, Gottstein and Kocks [21] have already established a correlation between DRX and dynamic recovery.

Two separate studies were undertaken on copper and nickel single crystals, which had been deformed in multiple slip to various, relatively large strains at various temperatures: some crystals underwent various recovery treatments and were then retested at the previous deformation temperature to establish the precise influence on subsequent strain-hardening behaviour; others were prepared into foils and annealed *in situ* in a high voltage electron microscope (HVEM) to gain insight into the dislocation rearrangement processes.

Two other studies of recovery in copper and nickel single crystals have previously been undertaken: van Drunen and Saimoto [24, 25] investigated recovery kinetics after multiple-slip deformation (primarily in $\langle 100 \rangle$ crystals); and Prinz *et al.* [26] observed recovery events *in situ* in an HVEM after deformation in single slip. Both sets

of authors interpret their results in terms of loop or dipole annihilation processes.

2. Mechanical tests

2.1. Copper

Tensile samples approximately 6 mm in diameter and 38 mm long were grown from the melt, with shoulders, in a $\langle 111 \rangle$ axial orientation [21]. A gauge section about 13 mm long was spark machined into these samples, in order to avoid premature recrystallization from the grips. The cross section was $3.5 \times 3.5 \text{ mm}^2$ in most cases, $6 \times 1.2 \text{ mm}^2$ in some. The specimens were deformed in an Instron tensile tester at a constant crosshead speed of 0.2 mm min^{-1} (corresponding to an initial shear strain rate of $5 \times 10^{-4} \text{ sec}^{-1}$) under a reducing atmosphere of 90% $\text{N}_2 + 10\% \text{H}_2$. Details of sample geometry and deformation procedures are given elsewhere [21].

In a first set of experiments, the aim was to duplicate the aluminium experiments at the same homologous temperatures: deformation at 180°C ($T_m/3$), annealing at 400°C ($T_m/2$). The annealing was done *in situ*, at zero load. Fig. 1 shows the results of two anneals, of 1/2 and 2 h, respectively*. In this experiment, as well as in others of the same kind, the deformation behaviour after recovery was always of Type I; in one of the

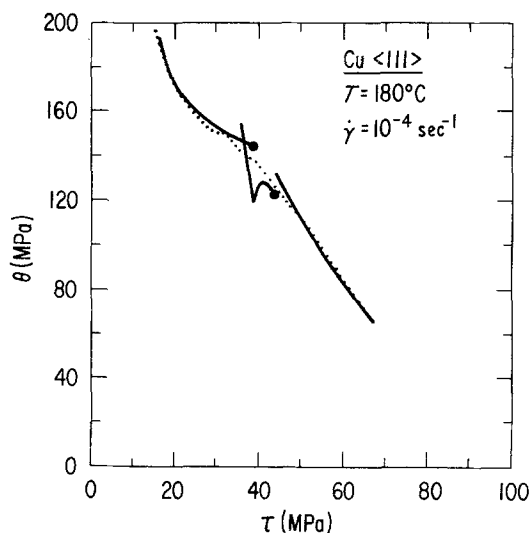


Figure 1 Hardening rate $\theta = d\tau/d\gamma$ of a copper $\langle 111 \rangle$ crystal deformed at 180°C , with intermediate anneals for 1/2 and 2 h at 400°C . The dotted line represents the curve for a continuously deformed sample. A final anneal for 2 h produced recrystallization.

*Heating and cooling took about 45 min each in addition.

cases displayed in Fig. 1, a very short initial transient with a lower-than-normal hardening rate was observed, which has the appearance of a reloading yield point [27] rather than of Type II recovery. After the end of the test shown in Fig. 1, recrystallization occurred during a two hour anneal.

In a second series of experiments, deformation was imposed at $T_m/2$ and repeatedly interrupted by hold times at zero load. Fig. 2 shows the results for one specimen, which was deformed with hold periods of increasing duration. Again, the behaviour was always of Type I, even though the last hold time was 17 h. After larger strains, the specimen recrystallized dynamically.

Finally, some crystals were deformed near $0.75T_m$ and annealed at even higher temperatures. Fig. 3 shows that even here recovery was of Type I, and very little at that. Another specimen was deformed to a stress marked by A in Fig. 3 and annealed for 7 h at 874°C : it recrystallized*.

In summary, all attempts at finding macroscopic Type II recovery behaviour in copper failed.

2.2. Nickel

The nickel crystals were grown with a $\langle 411 \rangle$

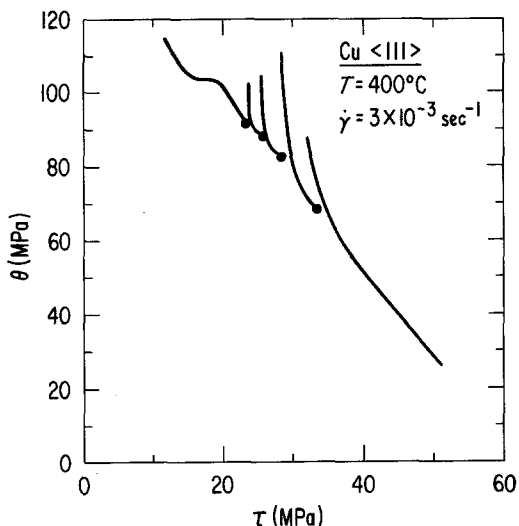


Figure 2 Hardening rate of a copper $\langle 111 \rangle$ crystal deformed at 400°C , with multiple interruptions: at each of the stresses marked by a heavy dot, the specimen was unloaded, held for increasing periods, and reloaded. Hold times: 0, 1/4, 1/2, 17 h. At the end, the specimen recrystallized dynamically.

*Dynamic recrystallization occurred at the end of the test shown in Fig. 3, at a stress equal to 0.94 of the saturation stress. This provides an interesting additional data point for Fig. 9 of Gottstein and Kocks [21], confirming their conclusion that $0.75 T_m$ is a critical transition temperature.

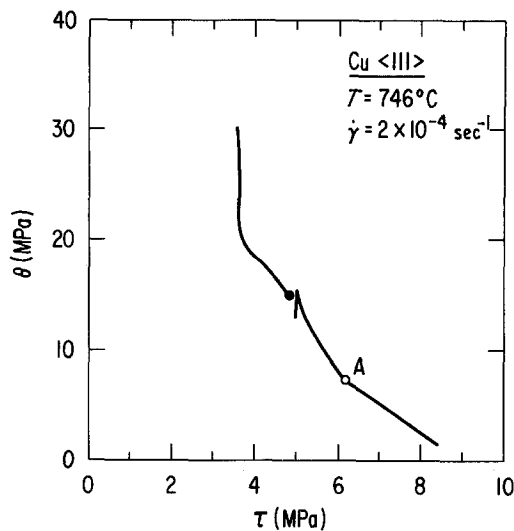


Figure 3 Hardening rate of a copper $\langle 111 \rangle$ crystal deformed at 746°C with one intermediate anneal for 2 h at 840°C . Another crystal, deformed to point A, recrystallized during 2 h at 874°C .

orientation by the floating-zone technique; they were welded to polycrystalline nickel shoulders [21]. A square gauge section of 3.2 mm edge length, 13 mm long, was sparked into them. They were deformed at a constant crosshead speed of 0.2 mm min^{-1} in an atmosphere of 90% N_2 and 10% H_2 . They exhibited uniform double slip.

Deformation at 300°C ($T_m/3$) revealed jerky flow; presumably, the crystals contained impurities. One crystal was alternately deformed at this temperature and at 600°C ($T_m/2$) and also annealed at the latter temperature. To the extent that any recovery could be identified at all, it was of Type I.

Another crystal was strained at $T_m/2$ (where deformation was smooth) and held repeatedly at the same temperature under zero load, like the second series of copper crystals above. Even after 18 h, recovery was of Type I (Fig. 4). A final crystal was deformed at the same temperature and annealed at 700°C for 18 h; it still exhibited Type I recovery. None of these specimens ever recrystallized, statically or dynamically: they formed a chisel-type neck. It is an interesting question that deserves further study, whether this was due to the impurities or the orientation; $\langle 111 \rangle$ crystals of the same nickel, but grown somewhat differently, did show both static and dynamic recrystallization under similar circumstances [21].

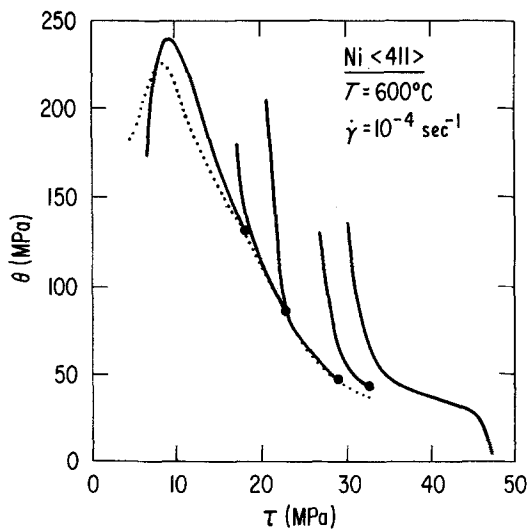


Figure 4 Hardening rate of a nickel $\langle 111 \rangle$ crystal deformed at 600°C , with multiple interruptions (as in Fig. 2). Successive hold times: 3/4, 2, 6, 18 h.

3. HVEM *in situ* annealing experiments

3.1. TEM specimen preparation and deformation

All the copper and nickel crystals used for transmission electron microscopy (TEM) investigations were oriented with a $\langle 111 \rangle$ tensile axis and had a sparked gauge section of 13 mm length with a cross section $6 \times 1.2 \text{ mm}^2$. The wide face was parallel to a $\{112\}$ plane. Tensile deformation was conducted in a reducing atmosphere of 90% $\text{N}_2 + 10\% \text{H}_2$ at $T_m/2$ (400°C for copper, 600°C for nickel). One nickel sample was deformed at 680°C . Details of sample geometry and deformation procedure are given elsewhere [21].

The copper samples were deformed to a resolved shear stress of 46 MPa (resolved shear $\gamma = 0.42$) which corresponds to 0.96 of the DRX stress. The nickel samples were deformed to a resolved shear stress of 77 MPa ($\gamma = 0.93$) which is equal to the DRX stress, since the samples did undergo partial dynamic recrystallization. The nickel sample that was deformed at 680°C recrystallized partially at a resolved shear stress of 45 MPa.

After deformation the gauge section of the deformed specimens was separated from the grip ends and two slices of about 0.5 mm thickness parallel to the $\{112\}$ side face were prepared from it by wire spark-cutting. These slices were chemically polished in a solution of 20 g CuSO_4 in 100 ml 70% HNO_3 (nickel), or in a solution of equal parts of 70% HNO_3 , acetic acid, and 85% H_3PO_4 (copper) to a final thickness of about

0.3 mm to remove the layers damaged by spark cutting. TEM specimens were prepared by spark-repanning discs from the polished slices followed by chemical polishing and then electropolishing to perforation. The electropolishing solutions were as follows:

Nickel: jet polishing in 400 ml H_2O , 300 ml glycerine and 400 ml H_2SO_4 at 8°C .

Copper: rapid initial thinning in Disapol D2 (recipe provided by Struers) at 8°C followed by jet polishing in 60% H_3PO_4 at 8°C .

The TEM specimens were mounted in the hot stage of an HVEM (AEI-EM7); which allowed rapid heating to a maximum temperature of about 800°C . The foil normal was $\{112\}$ and the specimens were only slightly tilted for best contrast conditions in bright field at 800 and 1000 kV for copper and nickel, respectively. The $\{112\}$ diffraction pattern was maintained in all tilt positions.

3.2. As-deformed structure at $\tau \approx \tau_R$

At $0.5T_m$, both copper and nickel have the same reduced dynamic recrystallization stress $\tau_R/\mu = 1.32 \times 10^{-3}$ (shear modulus $\mu = \{c_{44}[(c_{11} - c_{12})/2]^{1/2}\}$), although the absolute values of their corresponding flow stresses differ widely. The dislocation structure of both specimens is depicted in Fig. 5, showing the dislocations arranged in tangled cell walls which enclose predominantly equiaxed cell volumes. Some cells are narrow and elongated parallel to the trace of at least one slip plane and contain diffuse bands of accumulated dislocations. The orientation difference between adjacent cells was found to be small and to vary randomly. The scale of the cell size was very similar for both copper and nickel with an average linear intercept of $1.5 \mu\text{m}$. This result confirms the frequently stated conclusion that the subgrain size is essentially a function of τ/μ , independent of material and deformation history [28–30]. The data for copper are in good agreement with the results of Wantzen [31] for $\langle 111 \rangle$ single crystals.

In order to compare the effects of static recovery with those of dynamic recovery, one nickel specimen was investigated that had been deformed at a slightly higher deformation temperature ($680^\circ\text{C} = 0.55T_m$). The corresponding substructure is presented in Fig. 6. The overall appearance is similar to the structure obtained at 597°C . The cell morphology reveals a mixture of large, approximately equiaxed cells and small

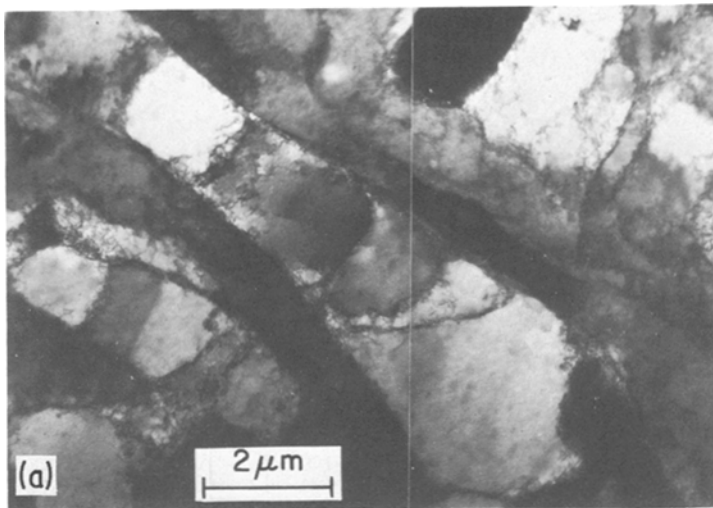
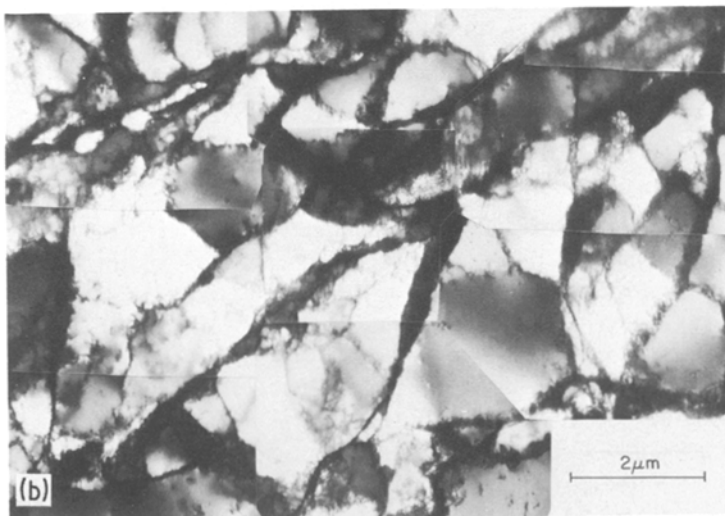


Figure 5 (a) TEM micrograph (at 100 kV) of a deformation structure in a copper $\langle 111 \rangle$ crystal at the recrystallization temperature for a deformation stress for a deformation temperature of $0.5 T_m$: $T = 405^\circ \text{C}$, $\tau = 46 \text{ MPa}$. After [21]. (b) As Fig. 5a, for nickel: $T = 597^\circ \text{C}$, $\tau = 77 \text{ MPa}$.



elongated cells which extend roughly parallel to the traces of the active glide planes. The dislocation structure still exhibits predominant cell character and heavily tangled dislocation arrangements. In comparison to lower deformation temperatures, however, the cell walls appear sharper; locally, well defined sub-boundaries are observed.

One interesting example is marked by A in Fig. 6. It is easily recognized as a sharp boundary by its fringe contrast, which is perturbed locally by additional, "random" dislocations. Although no orientation measurement was made across this boundary, the random check of orientations within the investigated area did not reveal any major orientation differences; thus we conclude that it is a small-angle boundary. Also it is worth noting that the boundary is different from the adjacent cell walls by its strong curvature and

twist. This observation suggests that the boundary accommodated to internal stresses and to boundary tension at nodes with adjoining boundaries. This observation is significant, because it gives evidence that a sub-boundary can adjust its position; in other words, it is able to migrate.

3.3. Isothermal annealing experiments

An annealing treatment of a nickel specimen at 100°C below the deformation temperature ($T_m/2$) did not result in a noticeable change of the overall dislocation arrangement. Even when annealing at the deformation temperature, the structural changes are small within 4 h, which is 20 times the time of deformation (Fig. 7). With increasing annealing time, some thick cell walls became sharper and less tangled (A in Figs. 7a and b). Regular dislocation patterns did not develop

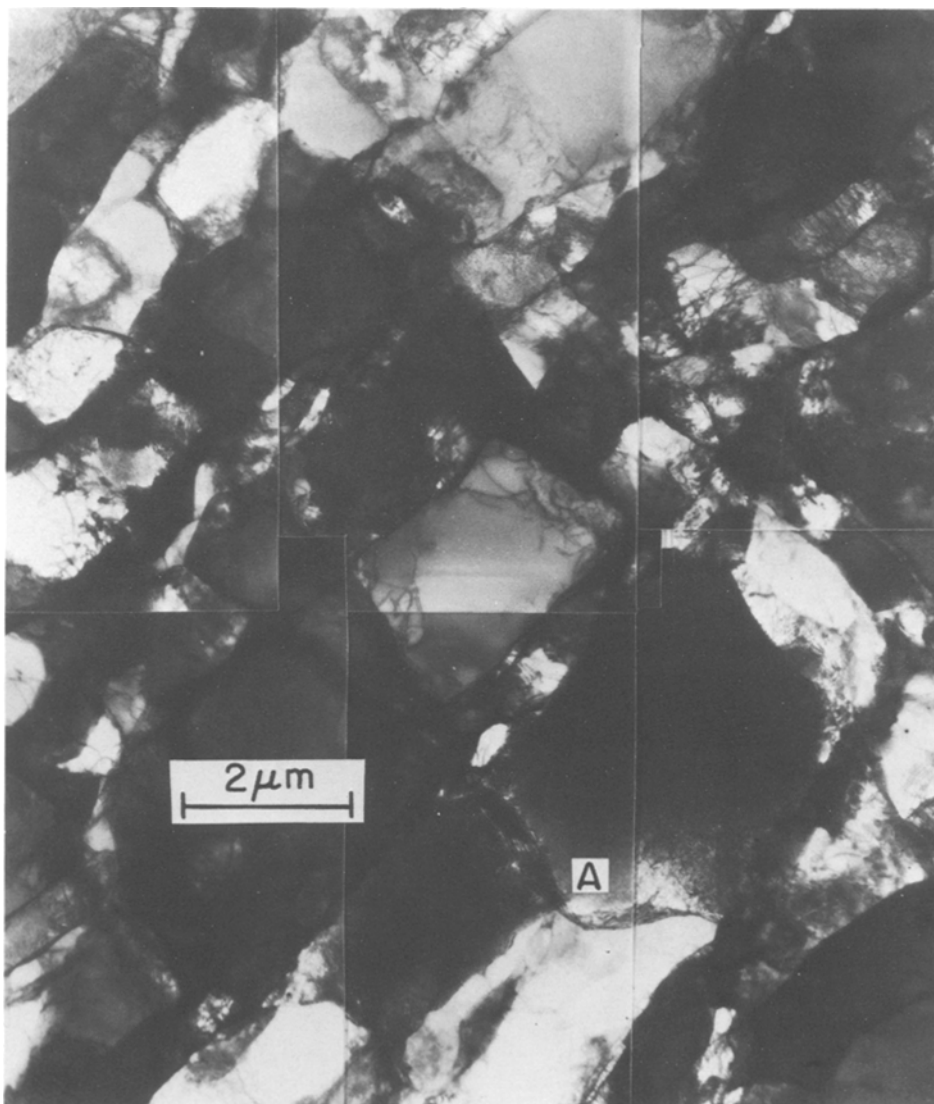


Figure 6 TEM micrograph (at 1 MV) of a $\langle 111 \rangle$ nickel crystal deformed at 680°C to the recrystallization stress, 45 MPa.

universally, although their local appearance was indicated (B in Fig. 7).

After 1 h at 700°C ($= 0.57T_m$) the nickel specimen displayed considerable ordering of the dislocation structure (Fig. 8b): locally sharp sub-boundaries and regular networks of dislocations as small-angle grain boundaries are developed. The progress is locally different though, and some areas with highly tangled dislocation arrangements can still be observed. After 2 h, the previously tangled areas indicate definitely the rearrangement of dislocations and their knitting into networks (Fig. 8c).

The extent of rearrangement depends on material, as can be recognized by comparison of

Fig. 8 with Fig. 9, which depicts the progress of static recovery of copper at 660°C ($= 0.69T_m$). The dislocation structure in copper looks far less recovered after 15 min than in nickel after 1 h at $0.57T_m$: it still shows predominant cell character, while nickel appears to be on the verge of a subgrain structure at much lower homologous temperatures.

A comparison of the deformation structure of nickel at 680°C (Fig. 6) with an annealing structure at 700°C (Fig. 8b) reveals little difference, except that the average cell size in Fig. 8b is smaller by about a factor of 2, corresponding to the difference in flow stresses. Locally defined sub-boundaries exist in an overall cell structure; if

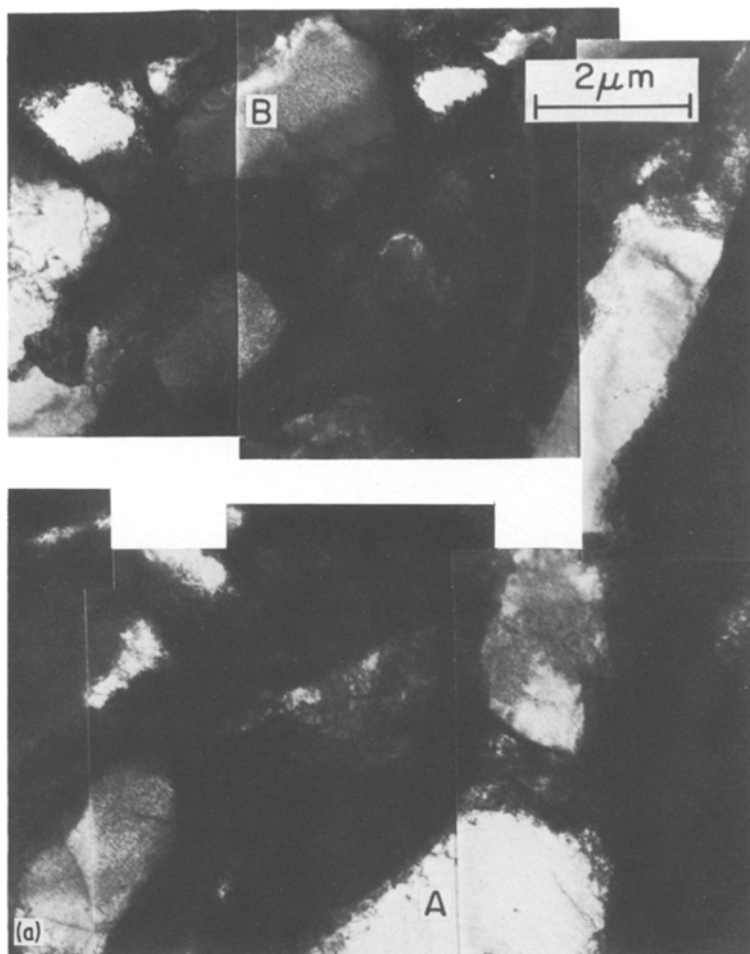


Figure 7 (a) TEM micrograph (at 1 MV) of a $\langle 111 \rangle$ nickel crystal deformed at 597° C to the recrystallization stress of 77 MPa: as-deformed structure. (b) As Fig. 7a: after *in situ* annealing at 600° C for 4 h.

anything, the cell walls in the unrecovered specimen are a little sharper. Note, however, that the total deformation time for the specimen in Fig. 6 was less than half of the annealing time for the specimen in Fig. 8b. This supports the generally accepted concept that dynamic recovery proceeds much faster than static recovery [4].

The structural change during annealing* of copper at 730° C ($0.74T_m$) can be seen from Fig. 10. During heating to the annealing temperature, the TEM image underwent strong contrast changes at temperatures $T > 600^\circ\text{C}$, which had the appearance of extensive dislocation rearrangement, but could also have been due to bending under thermal

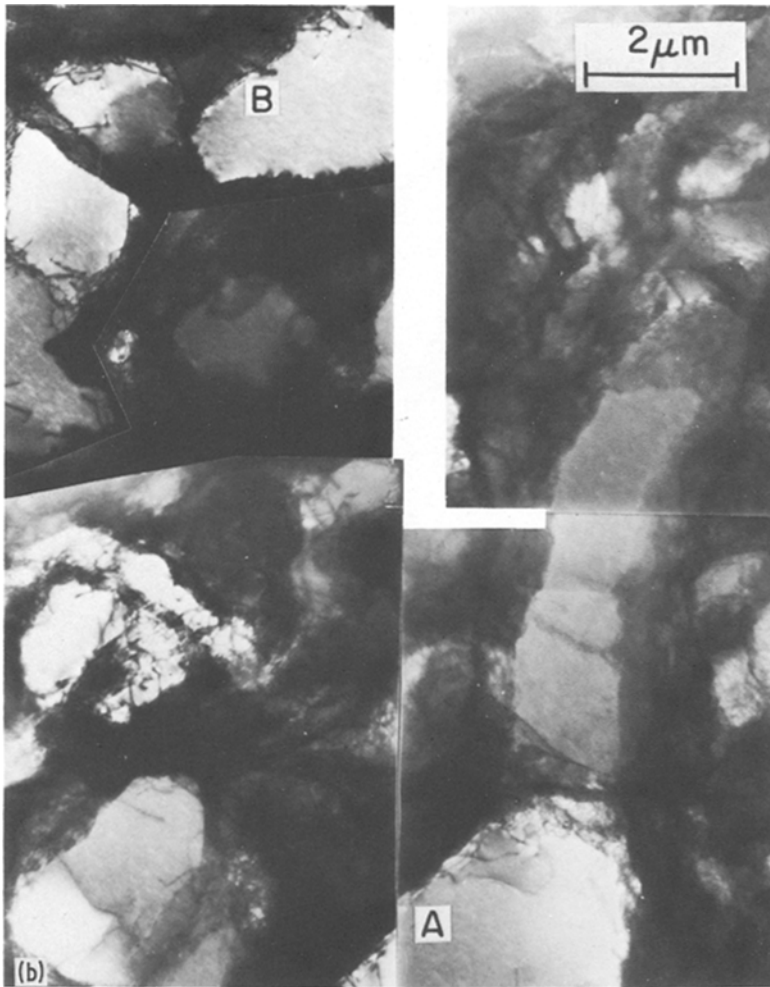
stresses†. While it is not certain that the structures shown before and after annealing belong to the same area, the qualitative differences in structure are evident. The tangled cell structure of the deformed state was converted into a subgrain structure containing regular dislocation arrays as in small-angle boundaries (an example is indicated by A) and networks of dislocations (B). The subgrain interior is virtually free of dislocations‡.

Since the highest feasible operating temperature of the hot stage was about 800° C ($0.62T_m$ for nickel), the 1 MeV beam was condensed sharply onto a nickel specimen at 790° C to provide enhanced recovery conditions. It was assumed

*The annealing was carried out in a reducing environment of 3 torr H_2 .

†It is noted that because of the unavoidable multi-beam conditions in the HVEM [32], the contrast reacts very sensitively to small orientation changes, which is particularly problematical for specimens with inhomogeneous orientations as in the present case. In other specimens, similar contrast changes have been observed at temperatures as low as 100° C as the result of bending.

‡Similar conclusions were reached from etch-pit studies of copper single crystals [33], and from X-ray diffraction studies of copper polycrystals [9].



that the focused beam would lead to a local heating of the specimen and the high point-defect production would enhance diffusion so that the procedure would correspond to annealing at a much higher although undetermined temperature. The result of this experiment is given by the sequence in Fig. 11.

Without the condensed beam the structure cleared very fast at 790° C and comprised clean sub-boundaries around essentially dislocation-free subgrain interiors (Fig. 11a). The diffuse bands of accumulated dislocations which frequently subdivide narrow and elongated subgrains (see also Section 3.2) were observed to move collectively. The subgrain arrangement is very much like the cell structure of the as-deformed material (Fig. 6) with respect to size and shape. Obviously the overall arrangement did not change in the process of conversion from a cell structure to a subgrain structure.

During prolonged annealing under the condensed beam, many dislocations were observed to leave the sub-boundaries and to sweep across the subgrain area marked A in Fig. 11b. Continued dislocation emission leads to the destruction of a boundary, which can be actually seen in Figs. 11b and c on the sub-boundary marked B.

In conclusion, enhanced recovery occurs by the fast transition of cell walls into sub-boundaries that may break up by continued dislocation emission.

4. Discussion

4.1. Type I recovery and dynamic recovery

The present experiments confirm the existence of Type I recovery over a wide range of conditions in copper and nickel single crystals deformed in multiple slip. All microscopic and macroscopic manifestations of this type of recovery were observed:

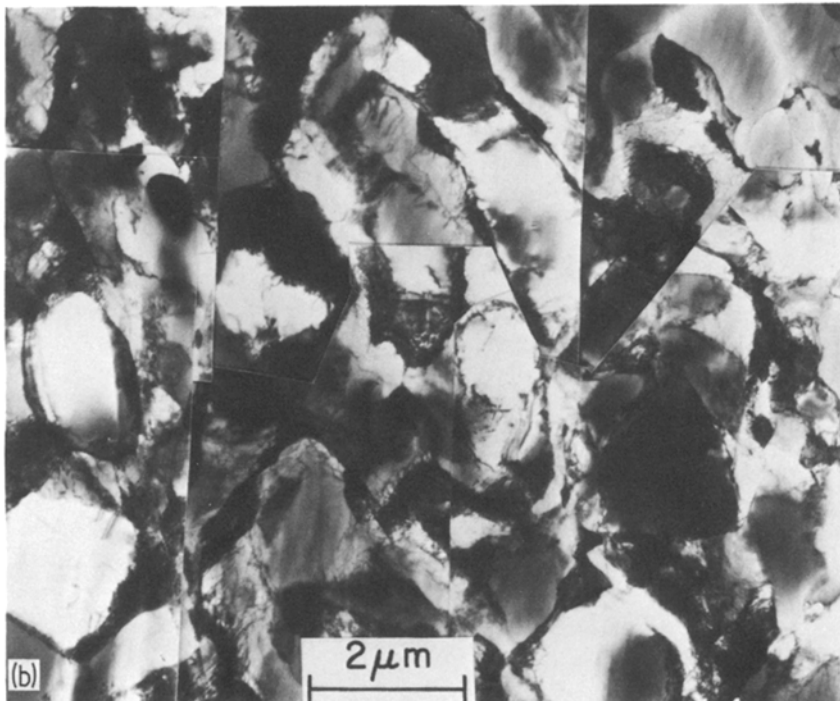
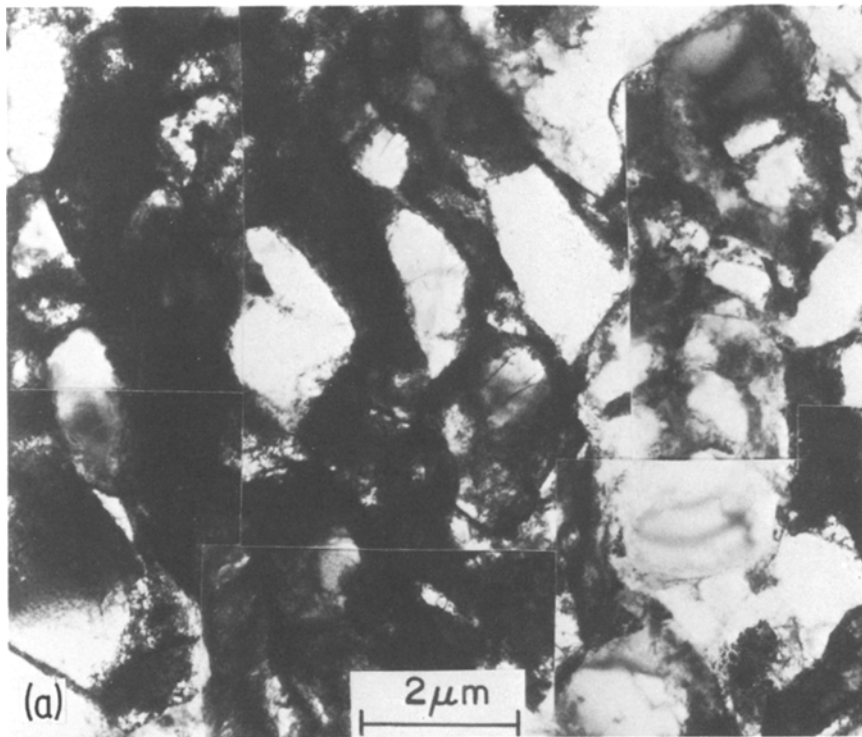


Figure 8 (a) TEM micrograph (at 1 MV) of a $\langle 111 \rangle$ nickel crystal deformed at 597°C to the recrystallization stress of 77 MPa: as-deformed structure. (b) As Fig. 8a: after *in situ* annealing at 700°C for 1 h. (c) As Fig. 8a: after *in situ* annealing at 700°C for 2 h.

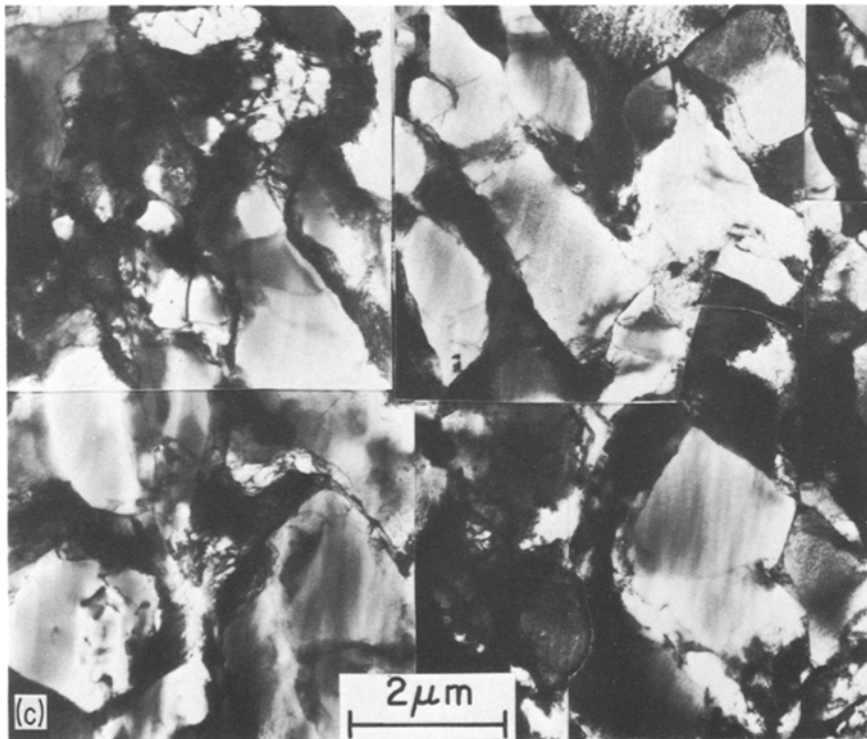


Figure 8 Continued.

1. the dislocation arrangement becomes gradually more cellular, with sharpening cell walls and cleaner cell interiors, until a subgrain structure is attained; the size and shape of the cells do not change during this process;

2. retesting at the previous deformation temperature evokes but a small transient in strain-hardening behaviour (with or without a small strain offset); and

3. the same substructure evolution occurs with strain during deformation without interposed annealing, i.e. with dynamic recovery [34].

These observations are in complete agreement with those made by Hasegawa and Kocks [3] on aluminium $\langle 111 \rangle$ single crystals (over a much narrower range of conditions, but in considerably more detail). Only two minor differences could be discerned:

1. Before the normal, gradual reloading transient, a very short initial region of lower-than-normal strain hardening appeared in many cases. This may well be in the nature of a reloading yield point [27], which is more prone to be seen in copper and nickel than in aluminium.

2. The appearance of partially sharpened cell

structures seemed to be more heterogeneous than in aluminium: small fragments of small-angle boundaries were imbedded in a generally cellular matrix (Figs. 9b and 10b). While there is always a spectrum of structural features present in deformed materials, such bold structural contrasts are not observed in hot worked material of high stacking fault energy like aluminium or α -Fe [28, 35, 36].

The latter observation may be significant in the context of the early stages of recrystallization. Gottstein and Kocks [21] have recently postulated that "nucleation" is always associated with a certain, if transient, degree of heterogeneity of the dislocation structure. At very high temperatures ($T > 0.75 T_m$ in copper and nickel), the nonuniformity is in the subgrain size [34]; at medium-high temperatures, the heterogeneity was proposed to lie in the degree of cell-wall sharpness [21], as it has been observed here for copper and nickel. Since this type of heterogeneity was not observed in aluminium [3], this is one argument that could explain the generally confirmed absence of DRX in aluminium.

A heterogeneity in the sharpness of cell walls might well be associated with high local stresses;

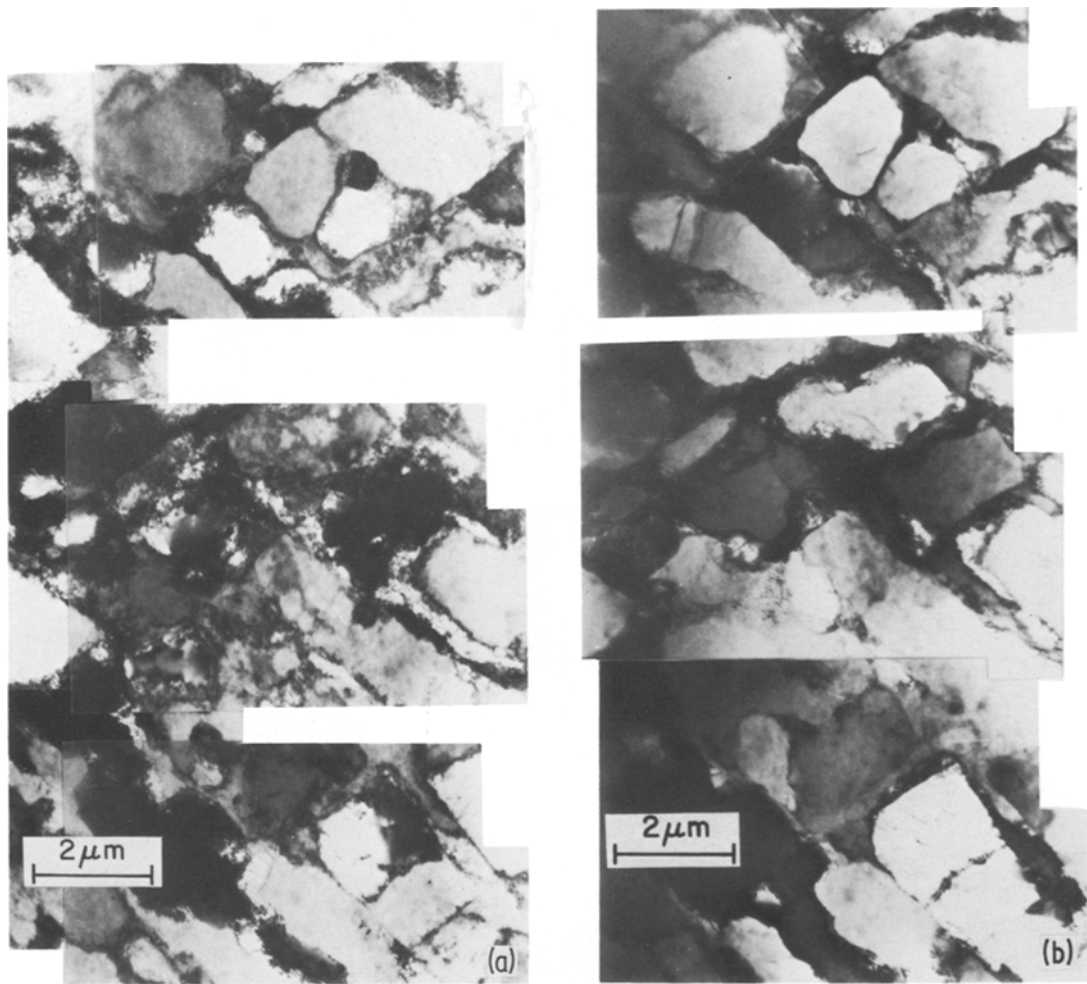


Figure 9 (a) TEM micrograph (at 800 kV) of a $\langle 111 \rangle$ copper crystal deformed to a shear stress of 46 MPa at 410°C : as-deformed structure. (b) As Fig. 9a: after *in situ* annealing at 664°C for 14 min.

in fact, these stresses were assumed to be responsible for the generally observed generation of twins during DRX at medium-high temperatures. An interesting question that arises from the present observation of these heterogeneities is whether the level of internal stresses is indeed higher in copper and nickel than in aluminium (even when normalized by the shear modulus, and at the same dislocation density).

4.2. Type II recovery, dynamic recrystallization and steady-state creep

The macroscopic manifestation of Type II recovery was stated by Hasegawa and Kocks [3] to be a long initial transient upon retesting at the deformation temperatures, which has the characteristic that it substantially under-

cuts the normal strain-hardening rate. In the present experiments, which extended to the largest possible prestrains (before dynamic recrystallization would occur) and to annealing temperatures of up to 880°C in copper and 600°C in nickel, this behaviour was never observed: either Type I recovery or recrystallization took place during annealing.

The microscopic mechanism of Type II recovery, as found by Hasegawa and Kocks [3] in aluminium, is the coarsening of an established clear subgrain structure, presumably by sub-boundary dissolution and/or migration. In the present investigation, sub-boundary migration was never observed in the HVEM, even at $T = 0.74T_m$ in copper (Fig. 10) or at $T > 0.62T_m$ in nickel (Fig. 11a). The absence of sub-boundary migration during HVEM *in situ* annealing, how-

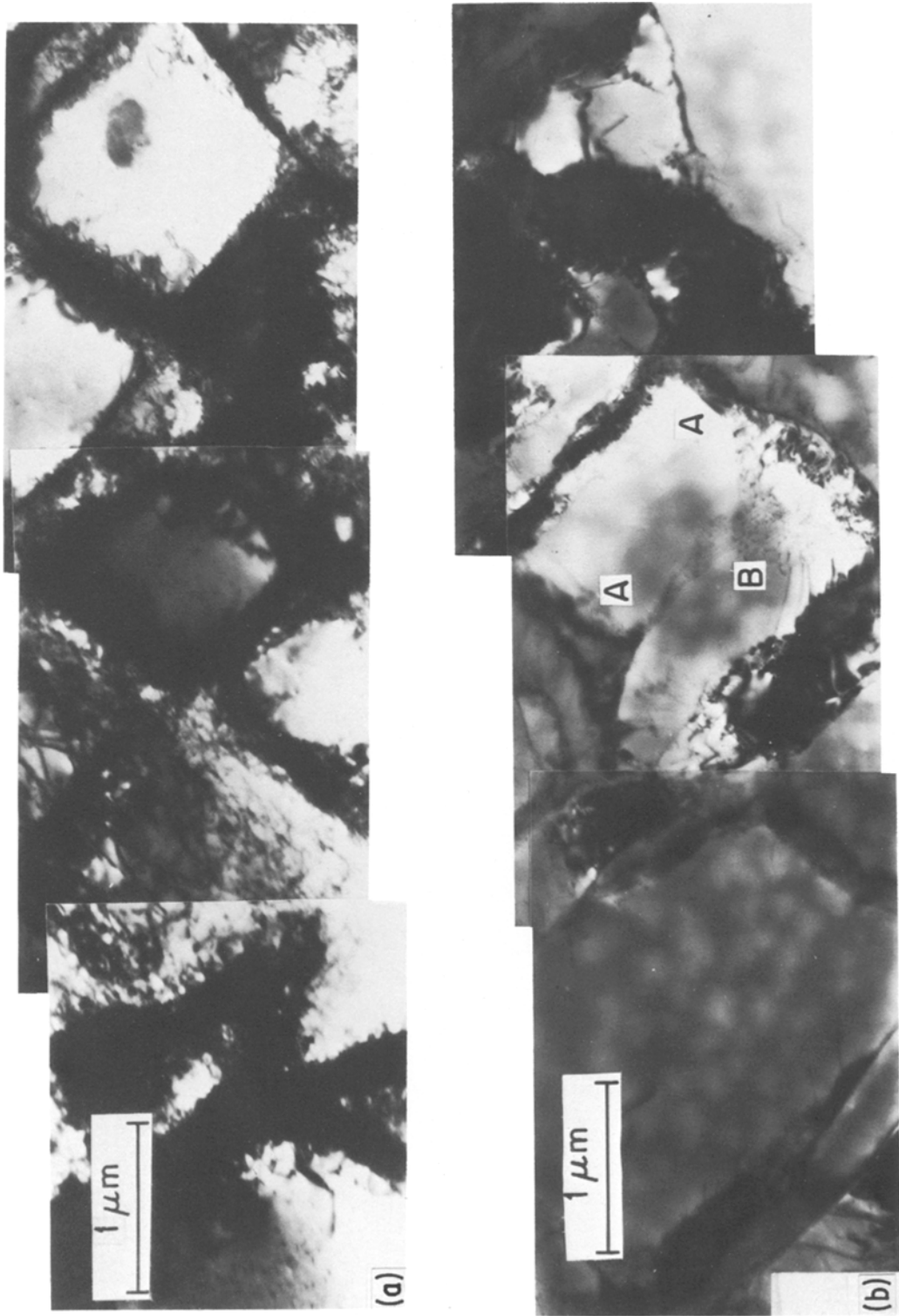


Figure 10 TEM micrograph (at 800 kV) of a $\langle 111 \rangle$ copper crystal deformed to a shear stress of 46 MPa at 40°C: as-deformed structure (a), and after *in situ* annealing at 730°C for 28 min (b).

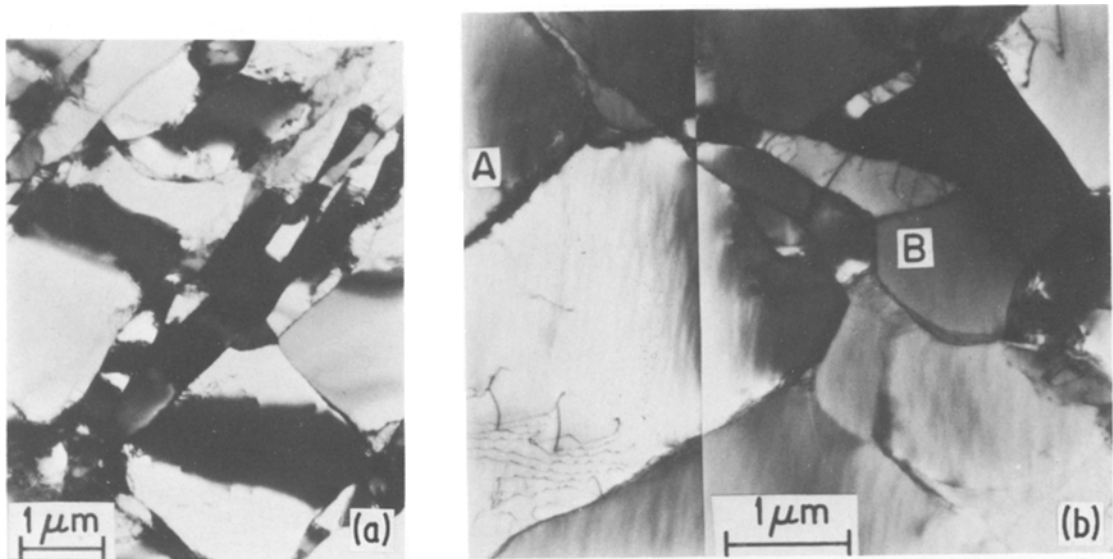
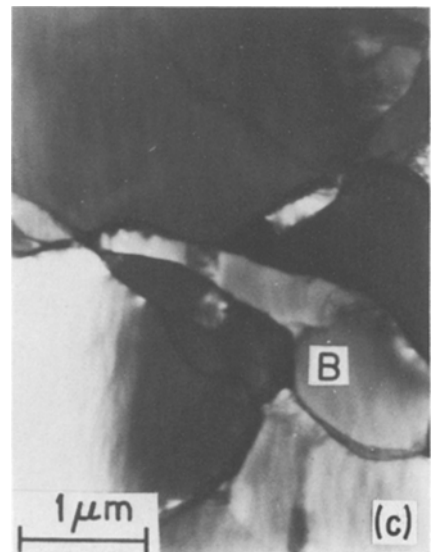


Figure 11 TEM micrograph (at 1 MV) of a $\langle 111 \rangle$ nickel crystal deformed to a shear stress of 45 MPa at 680°C: after *in situ* annealing at 790°C (a), and under the condensed beam (b, c).

ever, may be an artifact owing to the limited foil thickness that can be penetrated by 1 MeV electrons [5, 37]*. Some degree of mobility seems to be indicated by the observed sub-boundary curvature (Fig. 6) in the deformed structure at higher deformation temperatures ($T \geq 0.55 T_m$). Sub-boundary dissolution was observed in one case, in nickel under the condensed beam (Figs. 11b and c).

While substructure coarsening was, thus, not observed as a general phenomenon in this investigation, except it is catastrophic form during DRX, there are a number of other observations that suggest it to be a viable process in copper and nickel just as in aluminium. First, Karduck *et al.* [30] observed a strong broadening of the subgrain size distribution during deformation at temperatures in excess of $0.8 T_m$. This is similar to the bimodal distribution observed by Hasegawa and Kocks [3] after Type II recovery in aluminium.

Second, some mechanism of subgrain coarsening is presumably a prerequisite for the occurrence of high-temperature steady-state creep: to balance



the ongoing dislocation storage processes [38]. In this context, it is of interest to note that in the very regime where DRX occurs by catastrophic subgrain growth ($T > 0.75 T_m$), it occurs after steady-state deformation has in fact been achieved [21, 30, 39]. One must assume, then, that some fairly general subgrain coarsening process (balanced by refinement processes) must be going on before the instability occurs.

*This problem is considerably alleviated in aluminium which has a much higher transparency for electrons and therefore permits a foil thickness about ten times larger than for copper or nickel. The influence of the foil thickness is evidenced by the observation that the TEM specimens were always found to be recrystallized except for the transparent area. This indicates that even high-angle grain boundaries, which have a much higher mobility than low-angle grain boundaries, did not move into the transparent area.

We interpret these observations to mean that substructure coarsening occurs in all materials, but that the fluctuations, both spatial and temporal, that are intimately associated with this process lead to unstable growth in copper and nickel, but are stable in aluminium. This would explain why both static and dynamic recrystallization occur very soon after a clear, coarsenable substructure has been reached in the case of copper and nickel, but that in aluminium static recrystallization is sluggish (being replaced first by Type II recovery), and dynamic recrystallization absent. Type II recovery and the early stages of recrystallization are, then, two forms of the same process, namely subgrain coarsening. It remains to be explained why the stable form occurs in aluminium, at relatively low temperatures, and the unstable form in copper and nickel at very high temperatures*.

5. Summary

The static recovery behaviour of copper and nickel $\langle 111 \rangle$ single crystals deformed in multiple slip was investigated in mechanical tests and HVEM *in situ* annealing experiments. The results were compared with those of Hasegawa and Kocks [3] on aluminium $\langle 111 \rangle$ crystals, in which these authors found two distinct types of recovery. The major experimental results for both copper and nickel are:

1. Only the short Type I recovery transient was observed in mechanical tests after a multitude of annealing treatments on specimens predeformed to various levels; further increases in annealing time or temperature led to complete recrystallization, never to long Type II recovery transients.

2. HVEM *in situ* annealing below $0.6T_m$ revealed only the removal of dislocations from the cell interior and sharpening of the cell walls, which are associated with Type I recovery, and never the general coarsening of the subgrain structure associated with Type II recovery. The process of cell-wall sharpening appeared to be more heterogeneous than in aluminium.

3. One observation suggesting local sub-boundary mobility and one of sub-boundary dissolution are reported. The presence of a general substructure coarsening mechanism is, however, inferred

from other experiments: the broadening of the subgrain size distribution [30], and the observation of steady-state deformation before dynamic recrystallization at very high temperatures.

It is concluded that two types of dislocation rearrangement processes in fact exist in all materials. The process of cell-wall sharpening is similar in copper, nickel and aluminium, and leads to Type I static recovery and the type of dynamic recovery that is present even at low temperatures. A somewhat more pronounced heterogeneity of this process in copper and nickel could be responsible for the occurrence of dynamic recrystallization even in this regime.

The process of subgrain coarsening, whether by sub-boundary migration or dissolution, is intimately associated with fluctuations in size; these are unstable in copper and nickel, leading to dynamic recrystallization and to more rapid static recrystallization during annealing; they are stable in aluminium, leading to longer steady-state deformation and to Type II static recovery.

Acknowledgements

This work was supported by the US Department of Energy. G. Gottstein received additional support from the Deutsche Forschungsgemeinschaft.

References

1. U. F. KOCKS, *J. Eng. Mater. Technol. (ASME series H)* 98 (1976) 76.
2. F. J. HUMPREYS and J. W. MARTIN, *Phil. Mag.* 16 (1967) 927.
3. T. HASEGAWA and U. F. KOCKS, *Acta Metall.* 27 (1979) 1705.
4. U. F. KOCKS and H. MECKING, in "Strength of Metals and Alloys", edited by P. Hasen, V. Gerold and G. Kostorz (Pergamon, New York, 1979) p. 345.
5. T. E. TIETZ, C. L. MEYERS and J. L. LYTTON, *Trans. AIME* 224 (1962) 339.
6. J. E. BAILEY, "Electron Microscopy and Strength of Crystals" (Wiley, New York, 1963) p. 535.
7. R. A. VANDERMEER and P. GORDON, "Recovery and Recrystallization of Metals" (Interscience Publ., New York, 1963) p. 211.
8. E. C. W. PERRYMAN, in "Creep and Recovery" (ASM, Cleveland, 1957) p. 111.
9. W. G. TRUCKNER and D. E. MIKKOLA, *Metall. Trans.* 8A (1977) 45.
10. J. FRIEDEL, "Dislocations" (Pergamon, New York, 1964) p. 275.

*Mecking and Wantzen [40] have recently proposed that the difference can be explained on the basis of the driving force for growth: not only is the dislocation density achieved during deformation of aluminium lower, because of the high SFE and consequent rapid dynamic recovery, but also the energy stored for a given dislocation density is lowest in aluminium due to its small elastic constants.

11. R. W. CAHN, "Physical Metallurgy" (North-Holland Publ., Amsterdam, 1965) p. 925.
12. F. KIRCH, doctoral dissertation, RWTH Aachen (1970).
13. H. MECKING and G. GOTTSTEIN, in "Recrystallization of Metallic Materials" 2nd edn, edited by F. Haessner (Dr. Riederer-Verlag, Stuttgart, 1978) p. 195.
14. U. F. KOCKS, *Acta Metall.* 6 (1958) 85.
15. H. MECKING and U. F. KOCKS, *ibid.* 29 (1981) 1865.
16. T. HASEGAWA, T. YAKOU and U. F. KOCKS, *ibid.* 30 (1982) 235.
17. T. V. CHERIAN, P. PIETROWSKY and J. E. DORN, *Metall. Trans.* 185 (1949) 948.
18. T. H. ALDEN, *Metall. Trans.* 4 (1973) 1047.
19. G. GOTTSTEIN, D. ZABARDJADI and H. MECKING, *Met. Sci.* 13 (1979) 223.
20. P. J. T. STUITJE and G. GOTTSTEIN, *Z. Metallkd.* 71 (1980) 279.
21. G. GOTTSTEIN and U. F. KOCKS, *Acta Metall.* 31 (1983) 175.
22. G. GOTTSTEIN, J. BEWERUNGE, H. MECKING and H. WOLLENBERGER, *ibid.* 23 (1975) 641.
23. T. SAKAI, private communication (1982).
24. G. VAN DRUNEN and S. SAIMOTO, *Acta Metall.* 19 (1971) 213.
25. *Idem*, *Metall. Trans.* 10A (1979) 783.
26. F. PRINZ, A. S. ARGON and W. C. MOFFATT, *Acta Metall.* 30 (1982) 821.
27. P. HAASEN and A. KELLY, *Acta Metall.* 5 (1957) 192.
28. H. J. McQUEEN and J. J. JONAS, in "Treatise in Materials Science and Technology" Vol. 6, edited by R. J. Arsenault (Academic Press, New York, 1975) p. 393.
29. W. BLUM, doctoral dissertation, University Erlangen (1978).
30. P. KARDÜCK, G. GOTTSTEIN and H. MECKING, to be published.
31. A. WANTZEN, doctoral dissertation, TU Hamburg-Harburg (1982).
32. G. THOMAS and M. J. GORINGE, "Transmission Electron Microscopy of Materials" (Wiley, New York, 1979).
33. T. HASEGAWA, S. KARASHIMA and R. HASEGAWA, *Metall. Trans.* 2 (1971) 1449.
34. P. KARDÜCK, doctoral dissertation, RWTH Aachen (1981).
35. H. J. McQUEEN, *Trans. Jpn. Inst. Met. Met.* 9 (Suppl., 1968) 170.
36. J. P. A. IMMARIGEON and J. J. JONAS, *Acta Metall.* 19 (1971) 1053.
37. W. B. HUTCHINSON and R. K. RAY, *Phil. Mag.* 28 (1973) 953.
38. D. CAILLARD and J. L. MARTIN, in "Creep and Fracture of Engineering Materials and Structures", edited by B. Wilshire (Pineridge Press, Swansea, 1981) p. 17.
39. G. GOTTSTEIN, submitted to *Met. Sci.*
40. A. WANTZEN and H. MECKING, unpublished research, (TU Hamburg-Harburg).

*Received 29 December 1982
and accepted 20 January 1983*